On-demand dissolution of modular, synthetic extracellular matrix reveals local epithelial-stromal communication networks

Citation: Valdez, Jorge, Christi D. Cook, Caroline Chopko Ahrens, Alex J. Wang, Alexander Brown, Manu Kumar, Linda Stockdale, et al. "On-Demand Dissolution of Modular, Synthetic Extracellular Matrix Reveals Local Epithelial-Stromal Communication Networks." Biomaterials 130 (June 2017): 90–103.

As Published: http://dx.doi.org/10.1016/J.BIOMATERIALS.2017.03.030

Publisher: Elsevier BV

Persistent URL: http://hdl.handle.net/1721.1/117633

Version: Final published version: final published article, as it appeared in a journal, conference proceedings, or other formally published context

Biomaterials 130 (2017) 90–103

Contents lists available at ScienceDirect

Biomaterials

journal homepage: www.elsevier.com/locate/biomaterials

On-demand dissolution of modular, synthetic extracellular matrix reveals local epithelial-stromal communication networks

Jorge Valdez [a], Christi D. Cook [a], Caroline Chopko Ahrens [a, b], Alex J. Wang [a], Alexander Brown [a], Manu Kumar [a], Linda Stockdale [a], Daniel Rothenberg [a], Kasper Renggli [a], Elizabeth Gordon [a], Douglas Lauffenburger [a, b, c], Forest White [a], Linda Griffith [a, d, *]

[a] Department of Biological Engineering, Massachusetts Institute of Technology, Cambridge, MA 02139, USA
[b] Department of Chemical Engineering, Massachusetts Institute of Technology, Cambridge, MA 02139, USA
[c] Department of Biology, Massachusetts Institute of Technology, Cambridge, MA 02139, USA
[d] Department of Mechanical Engineering, Massachusetts Institute of Technology, Cambridge, MA 02139, USA

ARTICLE INFO

Article history:
Received 12 January 2017
Received in revised form
19 March 2017
Accepted 21 March 2017
Available online 23 March 2017

Keywords:
Matrix
Biomaterials
Systems biology
Sortase
Signaling

ABSTRACT

Methods to parse paracrine epithelial-stromal communication networks are a vital need in drug development, as disruption of these networks underlies diseases ranging from cancer to endometriosis. Here, we describe a modular, synthetic, and dissolvable extracellular matrix (MSD-ECM) hydrogel that fosters functional 3D epithelial-stromal co-culture, and that can be dissolved on-demand to recover cells and paracrine signaling proteins intact for subsequent analysis. Specifically, synthetic polymer hydrogels, modified with cell-interacting adhesion motifs and crosslinked with peptides that include a substrate for cell-mediated proteolytic remodeling, can be rapidly dissolved by an engineered version of the microbial transpeptidase Sortase A (SrtA) if the crosslinking peptide includes a SrtA substrate motif and a soluble second substrate. SrtA-mediated dissolution affected only 1 of 31 cytokines and growth factors assayed, whereas standard protease degradation methods destroyed about half of these same molecules. Using co-encapsulated endometrial epithelial and stromal cells as one model system, we show that the dynamic cytokine and growth factor response of co-cultures to an inflammatory cue is richer and more nuanced when measured from SrtA-dissolved gel microenvironments than from the culture supernate. This system employs accessible, reproducible reagents and facile protocols; hence, has potential as a tool in identifying and validating therapeutic targets in complex diseases.

1. Introduction

The limitations of animal models for studying human disease and for predicting drug responses are driving efforts to capture complex human physiology *in vitro* with 3D tissues, organoids, and "organs on chips". Naturally-derived ECM gels (e.g. collagen, Matrigel, fibrin) are workhorses in cell biology as they elicit many appropriate phenotypic behaviors. However, the properties of native ECM are difficult to tune in modular fashion, and dissolution of these gels can require hours-long incubations in protease solutions. A spectrum of synthetic and semi-synthetic ECM hydrogels enabling modular control of cell adhesion, degradation, stiffness, and other properties, have illuminated the ways cell phenotypes *in vitro* are governed not only by ECM composition, but also ECM biophysical properties, such as matrix mechanics and permeability [1–5]. Such synthetic ECMs are emerging as tools to improve functionality and reproducibility of 3D *in vitro* models.

The extracellular matrix not only directly interacts with cells through adhesion receptors, but it also modulates paracrine and autocrine signaling through binding interactions with cytokines. Therefore, 3D *in vitro* models are especially attractive for modeling complex biological systems where reciprocal paracrine communication networks between different cell populations, such as the epithelium and stroma, regulate function in health and disease. Elucidating these interactions can therefore aid in developing potential targets for therapeutics [6,7]. For example, the tumor stroma

* Corresponding author. Department of Biological Engineering, Massachusetts Institute of Technology, 16-429, Cambridge, MA 02139, USA.
E-mail address: griff@mit.edu (L. Griffith).

http://dx.doi.org/10.1016/j.biomaterials.2017.03.030

has become a well-recognized facilitator of malignant phenotypes and contributor to therapy resistance in carcinomas [8–10], and aberrant stromal-epithelial crosstalk is observed in endometriosis [6,11–13].

An additional desirable feature of 3D *in vitro* systems used for analysis of paracrine signaling is rapid breakdown of the ECM to yield individual cells, distinct cell populations (e.g., stromal and epithelial cells), as well as the local cytokines and growth factors produced by the cells. Methods to avoid degradation of proteins and other macromolecules are desirable, not only to preserve cell surface receptors and soluble signaling molecules for analysis and quantification, but also because proteolytic cleavage of cell surface growth factors and receptors triggers near-instantaneous changes in signaling networks, altering the parameters under investigation [14–17]. Previously, synthetic ECM breakdown strategies using thermal [18], chemical [19], ionic shifts [20], photodegradation [21,22], and proteolytic degradation [23] have all been deployed to release cells, but these approaches are either relatively slow, have variable success in minimizing cell damage, or are limited in application to relatively thin tissues.

Here, we describe a new modular synthetic ECM that addresses a significant gap in functionality – facile, localized, and highly selective rapid dissolution to release cells for individual cell assays and to separate disparate cell populations (i.e., stromal and epithelial cells) for signaling studies. The approach is based on a simple modification of the crosslinking peptide to introduce orthogonal dissolution of prototypical polyethylene glycol (PEG) hydrogels by variants of *Staphylococcus aureus* Sortase A, which are readily expressed in high yield as recombinant ~ 20 kDa proteins [24–27]. Unless specified otherwise, all experiments were performed using the pentamutant version of Sortase A P94R/D160N/D165A/K190E/K196T (SrtA) reported by David Liu [24]. SrtA catalyzes a peptide exchange process of the general form: (R)-*LPXTG* + ***G***GG-(R′) = (R)-*LPXT****G***GG-(R′) + *G*. This transpeptidase reaction is now an established protein engineering tool, used to ligate large protein subdomains together or to link proteins with synthetic polymers [24,28,29]. The reversibility of SrtA-mediated reactions [28,29], which is a shortcoming in most protein engineering applications, led us to investigate whether SrtA mutants could be used to disassemble synthetic ECM crosslinked with defined peptides while preserving crucial extracellular signaling proteins. The SrtA transpeptidase reaction as implemented here involved an *LPXTG* motif embedded within the crosslink and an N-terminal glycine donor, soluble *GGG*, to effectively sever the crosslinks in a reaction that is highly selective, as very few mammalian proteins include the *LPXTG* motif [24–27,30].

Here, we report how we first defined a modular, synthetic, dissolvable ECM ("MSD-ECM") composition suitable for functional co-culture of epithelial and stromal cells, using the endometrium as a model epithelial-stromal interaction. We then investigated the kinetics of gel dissolution as a function of enzyme and substrate concentrations as well as gel crosslinking parameters, establishing a protocol that allowed rapid dissolution of MSD-ECM gels used for co-cultures. The dissolution protocol was used to study the effects of SrtA-mediated dissolution on viability and signaling properties of endometrial cells and an additional highly sensitive epithelial cell type, primary hepatocytes. After evaluating the robustness of the dissolution process with a quantitative assay of 31 cytokines, growth factors, and MMPs recovered from gels, we then compared the SrtA-mediated process to standard degradation with proteolytic enzymes. We then investigated the relative concentrations of these molecules as detected in the culture supernate compared to the local microenvironment in the gel, using quantitative recovery after dissolution. Finally, we demonstrated how the temporal evolution of the cytokine network activated in response to stimulation of endometrial epithelial-stromal co-cultures with an inflammatory cue, interleukin 1β (IL-1β), was revealed with greater depth and fidelity using measurements made on proteins recovered from the dissolved MSD-ECM gel, compared to measurements on proteins from the standard culture supernate.

2. Results

2.1. Functionalized PEG hydrogels crosslinked with peptide substrates for SrtA support endometrial stromal-epithelial co-cultures

Although functionalized PEG hydrogels have been used for epithelial [31], endothelial [32], connective tissue [33], and stromal cells [34], co-cultures of epithelial and stromal cells require tuning matrix properties to meet the needs of both cell types [35]. Hence, we first established an endometrial stromal and epithelial co-culture in functionalized PEG gels as a model of a complex, multicellular, 3D system that can be interrogated through SrtA-mediated gel dissolution. We built on our previous model of the endometrial mucosal barrier, in which we defined a functionalized PEG gel composition suitable for supporting functional viability of an endometrial epithelial monolayer cultured on top of encapsulated endometrial stromal cells [35]. For this work, we extended the investigation of gel properties to include SrtA-mediated dissolution, and focused on recreating a glandular co-culture by co-encapsulating epithelial and stromal cells within the functionalized PEG gels. In this work, multi-arm PEG macromers activated with vinyl sulfone (PEG-VS) were partially functionalized with the adhesion peptide *PHSRN-K-RGD* [36,37] and crosslinked with a defined peptide containing substrates for both endogenous matrix metalloproteinases (MMPs) and exogenous SrtA (see Methods for full sequences). Hydrogel crosslinks are therefore subject to both cell-mediated remodeling as well as on-demand dissolution via addition of SrtA and *GGG*. *PHSRN-K-RGD* is a peptide mimic of integrin $\alpha_5\beta_1$-binding domain in the 9th and 10th Type III repeats in fibronectin (FN) [28,38–40].

We previously observed that the *PHSRN-K-RGD* peptide enhanced epithelial and stromal behaviors (attachment to gels, epithelial monolayer properties) compared to the minimal peptide *RGD* [35]. In those studies, epithelial cells were cultured on functionalized gels. For the glandular model, we first investigated the influence of gel composition on response of encapsulated epithelial cells, comparing *RGD* to *PHSRN-K-RGD* at a range of concentrations. As a primary metric, we quantified epithelial acinar polarization and lumenization, as indicated by the apical localization of F-actin and hollowing of the cell spheroids (Fig. S1). We observed that *PHSRN-K-RGD* greatly enhanced polarization and lumenization frequency compared to *RGD* at nominal concentrations above 500 μM (polarization frequency is 81% for *PHSRN-K-RGD* compared to 78% for Matrigel and 44% for RGD, Fig. S1). For future experiments involving co-encapsulation, we therefore encapsulated the co-cultures by presenting *PHSRN-K-RGD* (2 mM nominal concentration). Endometrial epithelial cells (Ishikawa cell line) and primary human stromal cells were incorporated into the gel during crosslinking as described in *Methods*. We compare the behavior of the co-cultures in PEG gels to those encapsulated in the canonical standard natural ECM, Matrigel [1,41–45] as outlined schematically in Fig. 1A.

In synthetic ECM, epithelial cells proliferated and formed properly polarized, cytokeratin 18-positive ($CK18^+$) acinar structures characterized by apical localization of F-actin, while primary endometrial stromal cells ($CD10^+$) adopted a mesenchymal-like elongated phenotype (Fig. 1B). While Matrigel gels also facilitated polarized epithelial acini, elongated stromal cells were qualitatively

observed less frequently (Fig. 1B), consistent with other reports [41,42]. Although cells were encapsulated at the same seeding density in both hydrogel systems, the tendency for PEG gels to swell (1.5X-2X nominal volume) and Matrigel to compact upon cell contraction explains the effective difference in cell densities. Nevertheless, MSD-ECM elicits the phenotypes of interest at least as effectively as the Matrigel benchmark. In addition to corroborating that functionalized synthetic PEG gels supported the appropriate epithelial and stromal morphologies, we evaluated endometrial phenotypic behavior by inducing decidualization, a process wherein a subpopulation of the endometrial stromal cells respond to hormonal cues by plumping up and dramatically increasing production of characteristic proteins, including insulin-like growth factor binding protein 1 (IGFBP-1) and prolactin [46,47]. This decidualization functional assay revealed comparable responses in PEG and Matrigel hydrogel systems, as assessed by IGFBP-1 secretion in response to the canonical cues 8-Br-cAMP and medroxyprogesterone acetate (MPA) (Fig. 1C).

Altogether, these data suggest that functionalized PEG hydrogels adapted to include a peptide substrate for SrtA, thus providing potential for on-demand dissolution, are suitable for 3D epithelial-stromal co-cultures. As these gels are modular (components can be systematically mixed and matched, and properties tuned), synthetic (all components including peptides are chemically synthesized and can be purchased commercially) and dissolvable (as we demonstrate below), we refer to the general formulation as "MSD-ECM." These gels offer a more robust range of stromal physiological morphologies compared to the Matrigel system, and at least comparable performance phenotypically to Matrigel in terms of decidualization response. The endometrial co-culture model described here was thus subsequently used for analysis of protein communication networks in homeostasis and inflammation using

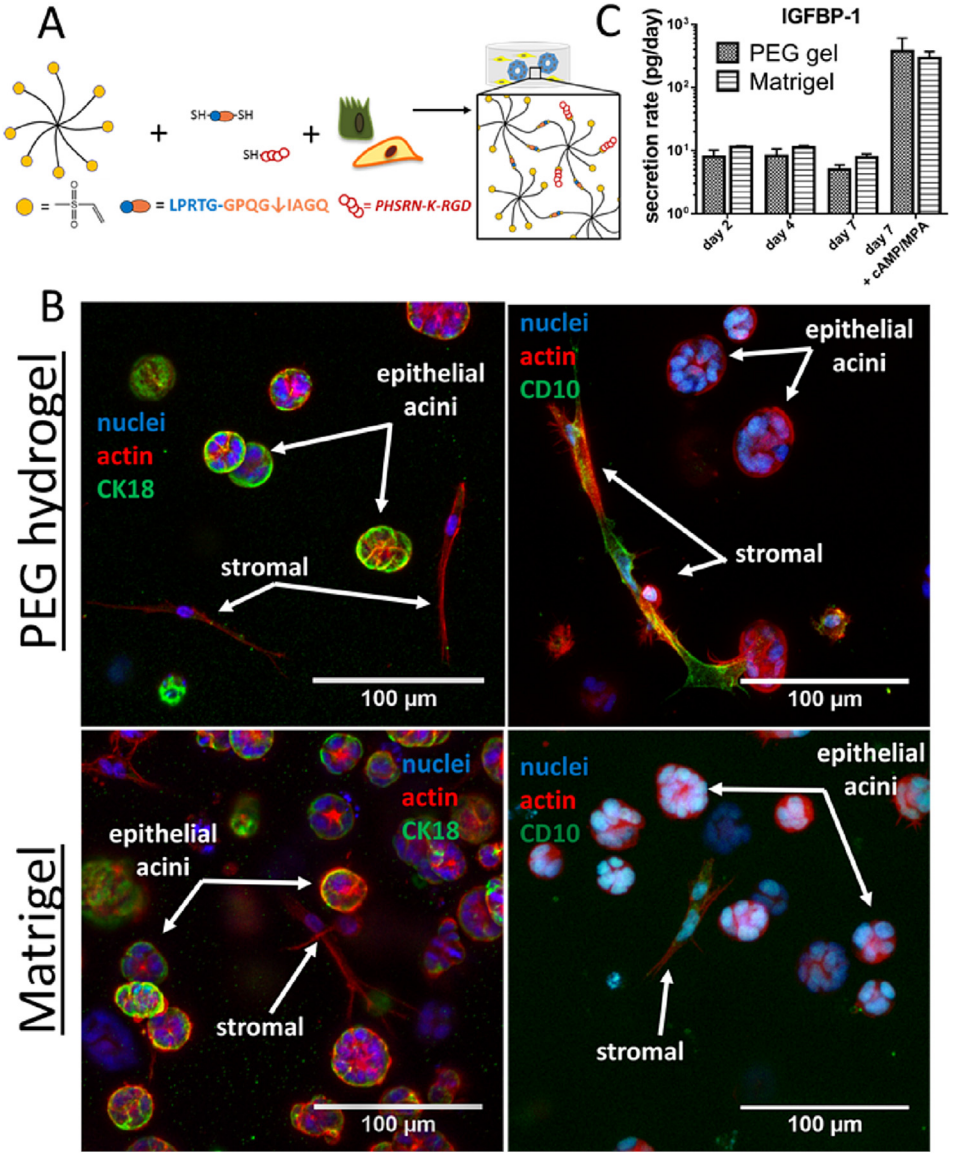

Fig. 1. SrtA-dissolvable hydrogels support functional stromal-epithelial co-cultures. *(A)* Gel encapsulation strategy using PEG vinyl sulfone (VS)/thiol chemistry (MSD-ECM) to crosslink and incorporate *PHSRN-K-RGD*. *(B)* 3D endometrial co-cultures of primary human stromal cells and epithelial (Ishikawa) cells. Confocal projections span 100 µm in the z direction. Composite images shown here obscure accurate evaluation of actin polarization in epithelial cells. Top row = PEG hydrogels (MSD-ECM), Bottom row = Matrigel. Red = actin (phalloidin), blue (DAPI), green as indicated. Scale bar = 100 µm. *(C)* IGFBP-1 basal and induction secretion rate of endometrial co-cultures in response to 8-Br-cAMP (0.5 mM) and medroxyprogesterone acetate (1 µM) added on day 4 in PEG and Matrigel gels. n = 4, error bars represent standard deviation.

the SrtA-mediated dissolution method described below.

2.2. MSD-ECM is rapidly dissolved by SrtA-mediated transpeptidation

The reversibility potential of SrtA (*S. Aureus*) chemistry can be a drawback in the context of protein ligation reactions, as desirable product can be further modified in the presence of N-terminal glycine substrates and is sensitive to hydrolysis [29]. However, we speculated that this behavior could be exploited to dissolve synthetic ECM hydrogels with an *LPRTG* motif incorporated into the gel crosslinks, as addition of SrtA together with soluble *GGG* drives a transpeptidase reaction that functionally severs the crosslink [28] (Fig. 2A). In order to establish kinetics of the dissolution process for a range of enzyme, substrate and MSD-ECM gel crosslinking parameter values, we synthesized gels incorporating fluorescently-tagged versions of the adhesive peptide *PHSRN-K-RGD* (see Methods) to monitor macromer release as a measure of gel dissolution (Fig. 2B).

We first tested dissolution of relatively large MSD-ECM gels (discs 1 mm thick with 4.7 mm diameter post-swelling) using a concentration of SrtA (pentamutant) at the upper end of the values reported for cell surface labeling (50 μM) and a concentration of soluble *GGG* of 18 mM, which is approximately 5-fold above the SrtA K_m for the N-terminal glycine substrate ($K_{M,\ GGG}$ = 2.9 mM [24]). This protocol resulted in complete gel dissolution in 14–17 min (Fig. 2C, open circles), and the gel appeared to shrink during dissolution, suggesting a surface erosion mechanism. SrtA (M_w = 17,860 Da) diffuses more slowly than *GGG* (Mw = 235 Da) and is catalytically required for crosslink cleavage, hence the dissolution with this protocol is likely limited by the time required for SrtA to penetrate the gel.

We therefore postulated that relatively rapid, homogeneous MSD-ECM gel dissolution could be accomplished by a two-step process: incubation in SrtA followed by addition of a relatively high external concentration of *GGG*. Indeed, addition of SrtA for 30 min prior to addition of *GGG* (final 50 μM SrtA and 18 mM GGG) resulted in gel dissolution at ~5 min after addition of GGG (Fig. 2C closed circles), with dissolution appearing to occur as a bulk breakdown rather than surface erosion. Some release of PEG macromer was observed during the SrtA incubation step, possibly due to the known ability of SrtA to catalyze hydrolysis under low glycine donor concentration conditions (Fig. 2D). Another possibility for the low level of SrtA-mediated reaction in the absence of *GGG* is that the 10% serum in the incubation medium may contribute N-terminal glycines arising from the natural proteolytic destruction of hormones such as GNRH [48]; however, background macromer release times were similar in serum-containing and serum-free media (Fig. S2A).

To refine the gel dissolution protocol, we examined a shorter pre-incubation time (10 min) before adding *GGG* (18 mM) and SrtA concentrations of 10 and 50 μM, and found gels dissolved in ~5 min at 50 μM SrtA and ~20 min at 10 μM SrtA (Fig. 2E). The dissolution kinetics are relatively unaffected by crosslinking chemistry (norbornene vs vinyl sulfone) and crosslinking density (65% vs 85%) (Figs. S2B–D) and are also insensitive to the MMP-degradable sequence adjacent to the *LPRTG* (SrtA-recognition) site (Fig. S2C). Interestingly, hydrogels of 65% and 85% crosslinking

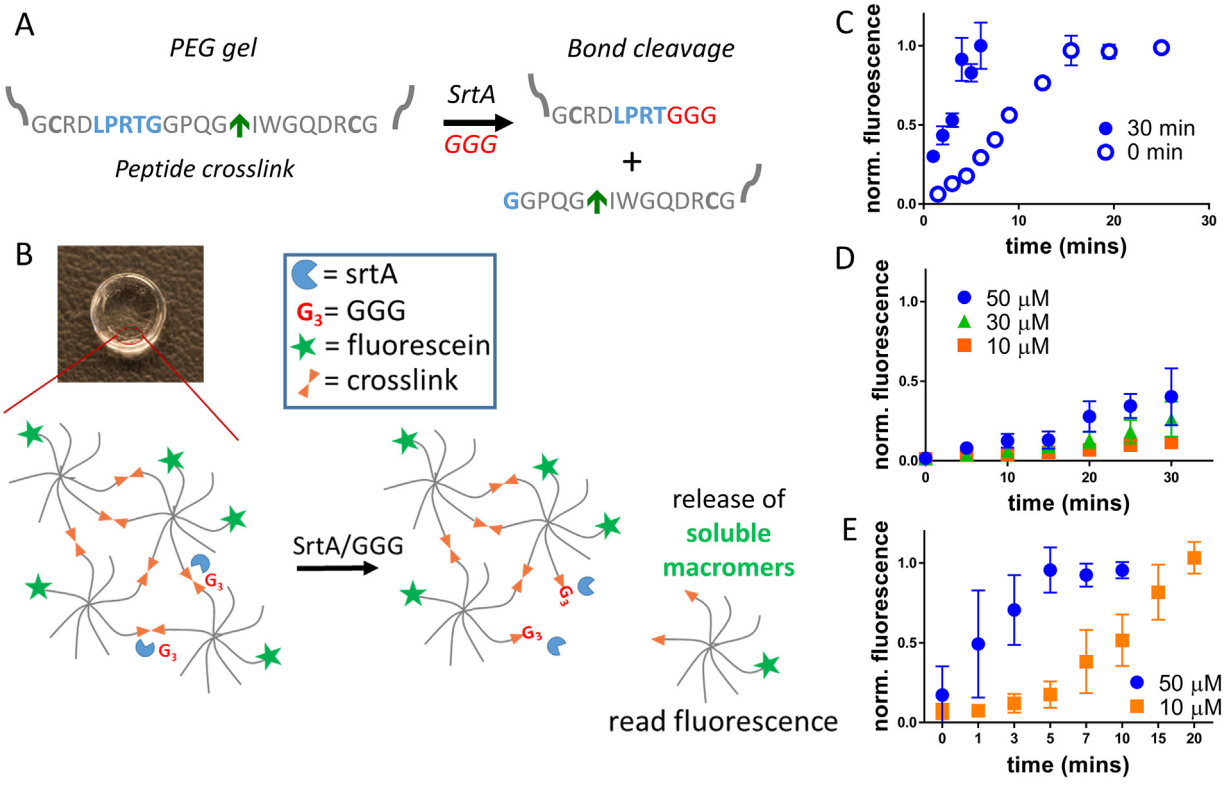

Fig. 2. SrtA-mediated hydrogel dissolution kinetics. *(A)* SrtA-mediated bond cleavage and hydrogel dissolution mechanism. Blue = SrtA substrate, red = soluble GGG, green arrow = MMP-sensitive sequence for cell-mediated remodeling. *(B)* Scheme of dissolution quantification assay through labeled macromer release (*F-PHSRN-K-RGD*). *(C)* Macromer release during gel dissolution after infusing a hydrogel with SrtA for 30 min prior to adding GGG, and by adding SrtA and GGG simultaneously (0 min). [GGG] = 18 mM, [SrtA] = 50 μM. *(D)* Macromer release during SrtA incubation in the absence of soluble GGG at 10, 30, and 50 μM. *(E)* Macromer release during gel dissolution upon GGG addition after 10 min incubation with SrtA at 10 μM and 50 μM. [GGG] = 18 mM. n = 3–4 PEG-NB gels, error bars represent standard deviation.

exhibited similar dissolution kinetics within the limits of resolution of the assay (Fig. S2D), perhaps because the greater dimensions of the more swollen gels (65% crosslinking) offset effects of the greater number of crosslinks (85% crosslinked gels), or the reaction is rate-limited by availability of *GGG*.

2.3. SrtA-mediated dissolution of synthetic ECM releases intact, viable, multicellular epithelial structures and stromal cells

SrtA has been widely used in the presence of mammalian cells without apparent effects on viability [25,26,49]. This is in agreement with a pilot experiment in which we observed that the viability of a human mesenchymal stem cell (MSC) line cultured on tissue culture plastic and exposed to MSD-ECM gels formed by SrtA was comparable to that of MSCs in gels formed by standard Michael-type addition gels. (Fig. S3). SrtA appears to have minimal effects on cultured MSCs, as it was present at a relatively high concentration of 338 μM during gel formation and culture. We also examined the possible effects of 30 min SrtA (0–50 μM) and *GGG* (0–18 mM) exposure on a more sensitive measure of cell response, activation of intracellular kinase signaling pathways. Using tumor cell lines with well-characterized signaling responses, we found no obvious intracellular kinase activation as measured by pan-phosphotyrosine western blot as well as by western blot of a highly sensitive intracellular kinase (ERK) and transmembrane receptor tyrosine kinase (MET) (Fig. S4). Finally, we used the well-known protein ligation properties of SrtA to encapsulate co-cultures of endometrial epithelial and stromal cells in synthetic gels functionalized with the *PHSRN-K-RGD* motif, and observed that cells encapsulated by this process behaved indistinguishably from those encapsulated by the standard Michael addition as assessed by morphology and response to decidualization cues (Fig. S5). Together, these experiments suggest that SrtA alone or in combination with *GGG* has no discernible effects on the cell types analyzed.

We next used the refined dissolution protocol (10 min incubation of 50 μM SrtA followed by 18 mM *GGG*) to dissolve the MSD-ECM of co-cultures comprising endometrial stromal and epithelial cells encapsulated in MSD-ECM, and cultured for a total of 11 days (Fig. 1). We compared the properties of cells released by SrtA dissolution to those of cells released by proteolytic (tryspin) degradation of identical cultures. To test the robustness of the cell release method, similar comparisons were made for rat hepatocyte MSD-ECM gel cultures as an epithelial cell type known to be sensitive to proteolytic degradation. Recovered cells were re-seeded onto tissue culture polystyrene (TCPS) and allowed to adhere overnight before fixing and staining them (Fig. 3A). Cell populations released by trypsin degradation contained a mix of single epithelial cells and stromal cells along with relatively few, small intact epithelial acini, consistent with the promiscuous degradation of both ECM and cell-cell adhesion junctions by trypsin (Figs. 3B and S7). In contrast, SrtA-mediated dissolution released intact epithelial acini along with individual stromal cells (Figs. 3B and S7), consistent with the relative lack of SrtA substrates in native mammalian proteins. Although we observed that a collagenase preparation (Liberase) also dissolved the synthetic gels while preserving cell-cell junctions while 3D-passaging epithelial spheroids (Fig. S6), the crucial metric for performance is recovery of viable cells together with the local proteins in the pericellular microenvironment within the gel, a metric explored in later experiments.

Single cells and epithelial acini re-plated onto TCPS after SrtA-mediated release from MSD-ECM showed strong positive immunostaining for endometrial epithelial (CK18, EpCAM) and stromal (CD10) markers and epithelial cells retained strong cell-cell junctions (Figs. 3B and S7). Similarly, rat hepatocyte aggregates recovered through SrtA dissolution and re-plated are larger compared to those recovered through trypsin degradation and exhibit defined actin filaments (Fig. S7C). Furthermore, SrtA gel dissolution allowed us to interrogate the local albumin concentration in the dissolved hepatocyte gel solution and compare it to the albumin concentration in the culture media at days 1 and 7. Fig. S7C shows that the concentration inside the hydrogel (measured from quantitative recovery after dissolving the gel) was approximately twice as high in the gel compared to the media at day 1, while at day 7, the concentration of albumin was similar inside and outside the gel (after correcting for volume differences and dilutions). Albumin is a relatively abundant protein, easily detected in the culture medium even though its concentration is lower there than in the gel microenvironment. However, this pilot experiment shows the potential of SrtA dissolution to reveal local protein concentrations, such as those of cytokines or growth factors, that may be present in the cell microenvironment but below assay detection limits in the culture supernate.

To illustrate the ability to recover cells for additional analysis, we released stromal-epithelial co-cultures 24 h after encapsulation and used flow cytometry to detect two distinct cell populations. Fig. S8 shows that the two populations ($CD90^+$ stromal, $EpCAM^+$ epithelial cells [50]) can be recovered and clearly distinguished from the functionalized 3D PEG gels. Results observed for SrtA-mediated and Liberase-mediated dissolution are comparable, while trypsin appears to modestly reduce the stromal marker (Fig. S8). Although the two surface markers evaluated here were not dramatically affected by trypsin or Liberase, many immune cell markers are highly sensitive to trypsin [51], thus motivating the use of the SrtA-mediated dissolution approach in future studies involving immune cell incorporation.

Although the dissolution process is relatively rapid (~5 min), intracellular kinase signaling states can change on that time scale and it is desirable to link intracellular and extracellular communication networks in some studies [14]. It is therefore desirable to freeze these states by lysing cells with RIPA buffer *in situ* before dissolving gels. Although analysis of intracellular signaling is beyond the scope of this study, we investigated the feasibility of such analysis by implementing a standard lysis protocol with RIPA buffer and then subjecting gels to the SrtA-mediated dissolution protocol (see Methods). We found that gel dissolution was unimpeded by the lysis step (Fig. S2E). Finally, analysis of cell surface-associated proteins by FACS, immunohistochemistry, or other methods likely requires a fixation step prior to dissolution to prevent dilution-mediated dissociation during cell recovery. We found that hydrogel-encapsulated cells that were cultured, then fixed with paraformaldehyde (PFA), were easily recovered by SrtA-mediated gel dissolution (Fig. 3C). Interestingly, stromal cells recovered from MSD-ECM gels after PFA fixation preserved their morphological states, including retention of actin filaments as revealed by phalloidin staining (Fig. 3C). Altogether these data suggest that the dissolution method is robust to a wide variety of MSD-ECM hydrogel properties and protocols commonly used for cellular analysis.

2.4. SrtA-mediated gel dissolution enables recovery of intact cell-produced proteins, enabling multiplex analysis of the temporal evolution of local cell-cell communication networks

Paracrine communication between stromal and epithelial cells regulates myriad tissue functions, but it is difficult to parse these extracellular protein networks in 3D culture. Measurement of molecules that escape into the culture supernate offers only partial representation of paracrine networks, as diffusion hinders gel/ECM escape, impairing estimation of local concentrations. Additionally,

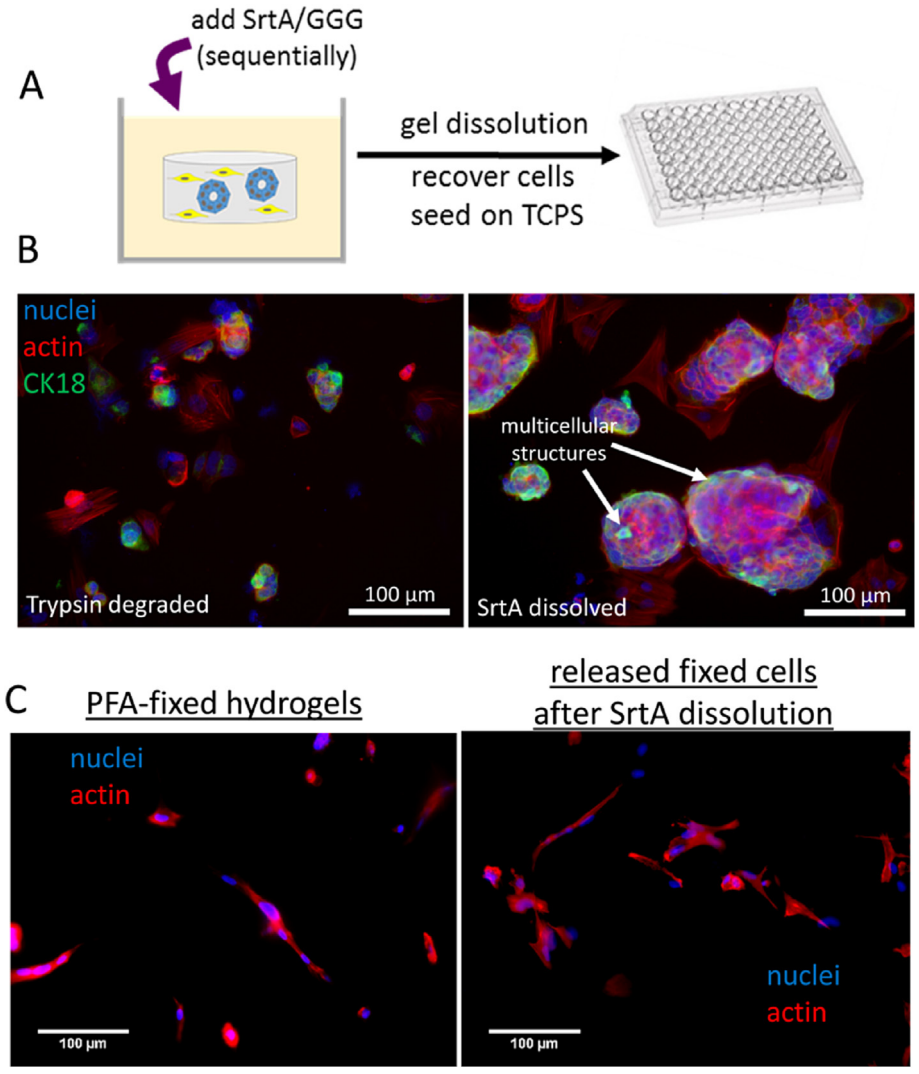

Fig. 3. SrtA-mediated hydrogel dissolution and cell recovery *(A)* Cell recovery from 3D gels and re-plating for staining. *(B)* Endometrial co-culture cells recovered from 3D functional synthetic gels and re-plated onto TCPS plates. Left = co-cultures recovered through trypsin degradation, right co-cultures recovered through SrtA-mediated dissolution. Arrows show examples of recovered acini. Blue: DAPI, red: phalloidin (actin), green: anti-cytokeratin 18. *(C)* Stromal cells fixed in 3D cultures, and then recovered through SrtA-dissolution of fixed hydrogels. Blue: DAPI, red: phalloidin. Scale bars = 100 µm.

local cellular consumption may greatly distort detection of the full spectrum of proteins present. Destruction of 3D matrices to recover local proteins by standard proteolytic degradation protocols also degrades many of the paracrine signaling proteins, such that they cannot be quantitatively analyzed by standard immunoassays. We postulated that SrtA dissolution would enable quantitative analysis of growth factors and cytokines in the extracellular environment and may reveal new features of local communication networks as they occur in real time.

We first compared the effects of the SrtA-mediated MSD-ECM gel dissolution protocol to standard proteolytic (trypsin and Liberase) degradation methods used for 3D tissues on the quantitative recovery of 27 cytokines and growth factors, using a multiplex bead-based immunoassay (Luminex) panel for analysis (see Methods). Dispase, which cleaves some basement membrane proteins along with N-terminal neutral amino acids and is commonly used to separate epithelial sheets from underlying stroma or to remove stem cells from substrates, was not included in the analysis as it is relative ineffective in degrading 3D stromal matrices [52]. Whereas about half the target proteins were undetectable after trypsin or Liberase incubation, incubation with SrtA rendered only IL-15 undetectable (Table 1). IL-15 is one of the very few human proteins containing an *LPXT* motif and is thus susceptible to the SrtA transpeptidase reaction.

Next, we used SrtA-mediated dissolution to discern whether the concentrations of cytokines, growth factors, proteinases, and their inhibitors measured in culture supernate outside the gel differed significantly from those measured in the local pericellular environment in the MSD-ECM. Endometrial epithelial and stromal cells were cultured for 48 h total in gels containing the adhesive peptide *PHSRN-K-RGD.* Twenty four hours after encapsulation, the co-cultures were stimulated with 10 ng/mL IL-1β (Fig. 4A). IL-1β is a strong inflammatory cue known to play roles in regulating endometrial decidualization, immune cell recruitment, and embryo implantation in the eutopic endometrium, and to be differentially expressed in endometrial peritoneal fluid and endometriotic lesion cells in numerous studies [53–55]. We observed that IL-1β treatment significantly diminished the secretion of decidual proteins

Table 1
Cytokine depletion after SrtA dissolution conditions, trypsin, and Liberase incubation.

Cytokine	% decrease following treatment		
	SrtA	Trypsin	Collagenase (Liberase)
Eotaxin	0	100	100
G-CSF	0	>70	100
IL-13	0	>20	100
IL-15	100	100	100
IL-17	0	>20	100
IL-2	0	100	100
IL-6	0	0	100
IL-7	0	0	100
IL-8	0	0	100
IL-9	0	100	100
IP10	0	0	100
CCL2 (MCP-1)	0	100	100
CCL3 (MIP-1α)	0	100	100
CCL4 (MIP-1β)	0	100	100
CCL5 (RANTES)	0	>10	100
VEGF	0	0	100

Unaffected: FGF-b, GM-CSF, IFN-γ, IL-10, IL12p70, IL-1β, IL-1ra, IL-4, IL-5, PDGFbb, TNFα.

prolactin and IGFBP-1 in primary proliferative phase endometrial stromal cells from three healthy donors (Fig. S9), suggesting that an inflammatory environment may contribute to diminished hormone-mediated decidualization observed in endometriosis, infertility and other endometrial pathologies, and is therefore a relevant cue to study.

The encapsulated epithelial cells present receptors for IL-1β [56]; therefore, we expected a robust inflammatory protein secretion response in response to IL-1β stimulation. To assess the response, gels were removed from the culture medium and dissolved to release cells and proteins contained in the gel, and the proteins were analyzed by Luminex (see *Methods*). The corresponding medium supernate samples were analyzed after being subjected to a mock dissolution process, in order to control for the possible influence of PEG macromers, peptides, SrtA, and *GGG* on the detection of target proteins by the Luminex assay (see *Methods* for dilution effects and calculation of concentrations). As expected, numerous cytokines and growth factors that were undetectable or found at relatively low, non-physiologic concentrations in the culture supernate were present at significantly higher concentrations within the gel, both under basal conditions before stimulation (Fig. 4B) and especially after 24 h of IL-1β stimulation (Fig. 4C), when we also detected substantial differences between several MMPs (Fig. 4C).

Notably, at 0 h (24 h after encapsulation), basal levels of basic FGF and IL-7 were below detectable levels in the culture medium, but were at detectable concentrations inside the gel where the cells can sense them (Fig. 4B). IL-12p70, IL-6, and basic FGF were among the cytokines that showed the most extreme discrepancies in gel and media concentrations after 24 h of IL-1β stimulation (Fig. 4C).

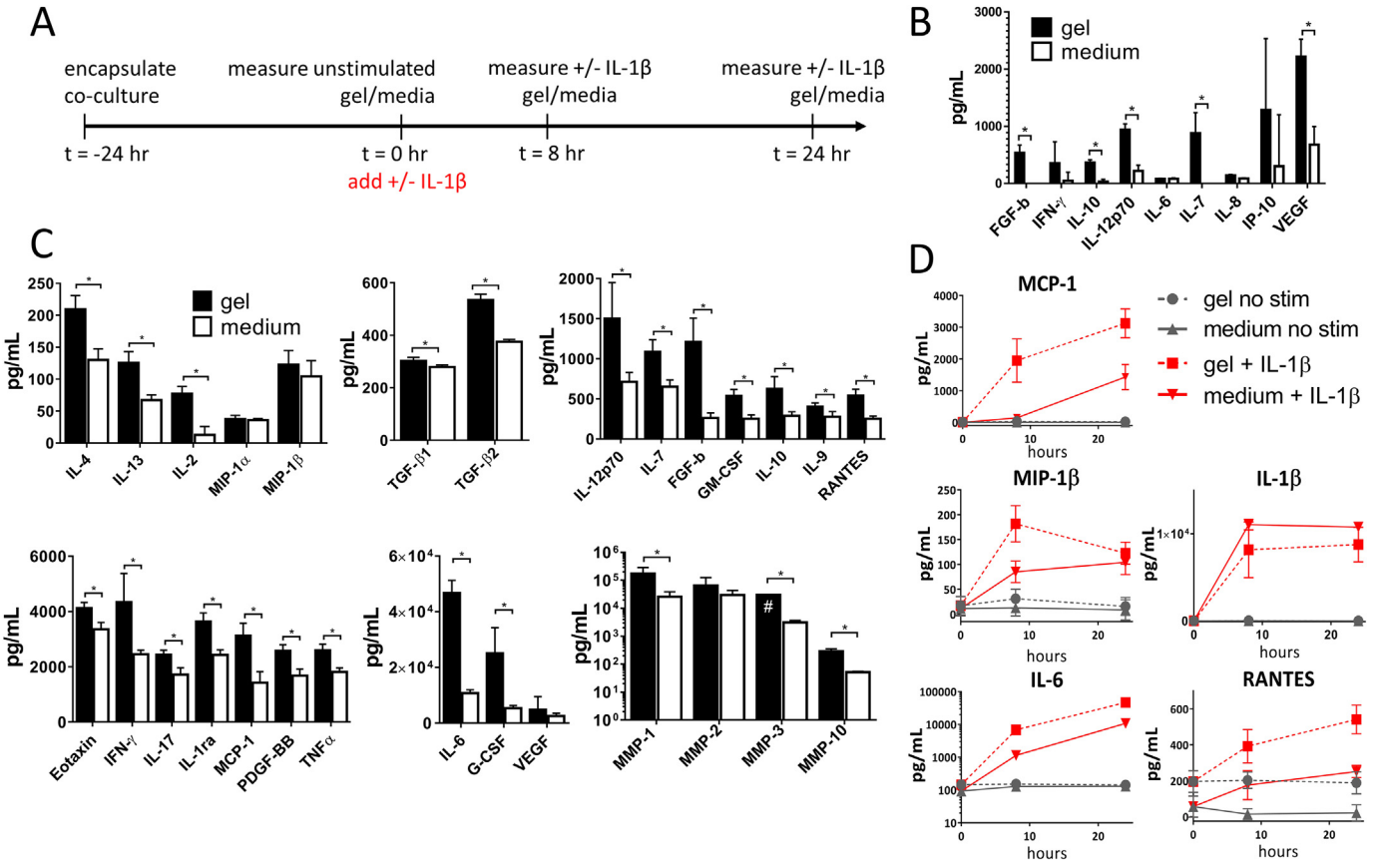

Fig. 4. SrtA-mediated dissolution allows for measurement of local cytokine dynamics at basal and inflammatory states. *(A)* Experimental timeline. *(B)* Local, in-gel (black) or external media (white) basal concentrations of the indicated proteins at 0 h. *(C)* Local, in-gel (black) or external media (white) concentrations of the indicated proteins at 24 h for conditions stimulated with IL-1β. Proteins are grouped according to similar scales of observed concentrations into a panel of graphs for clarity. # = signal above quantifiable levels and capped at 99.9% of highest point in standard curve *(D)* Dynamic temporal response of MCP-1, MIP-1β, IL-6, RANTES, and IL-1β concentrations inside the gel (dashed) and in culture media (solid). Red indicates conditions stimulated with IL-1β and grey indicates non-stimulated conditions. n = 9, error bars represent standard deviation. *$P < 0.05$.

This pattern is perhaps not surprising, as IL-6, IL-7 and FGFb are known to interact with glycosaminoglycans in the ECM and on the cell's surface [57–59]. Although diffusion plays a role in the retention time of these cytokines, the molecular weight (size) of measured proteins does not have a predictable influence on the ratio of external (medium)-to-local (in-gel) concentrations (Fig. S10), hence these discrepancies cannot be explained by a simple diffusion lag time analysis. These quantitative data underscore the intuitive prediction that measurements made on the culture supernate are poorly reflective of the complex dynamic changes within the local cell microenvironment, and that measurements made by dissolving the gel then quantitatively capturing released proteins reveals a more complete picture of the integrated temporal evolution of production, consumption, and ECM binding.

2.5. Local cytokine and growth factor measurements enhance temporal resolution and concentration fidelity of cell-cell communication networks

We next examined a more highly-resolved temporal response to an inflammatory cue, measuring in-gel and culture supernate concentrations at 0, 8 and 24 h after IL-1β (10 ng/mL) stimulation (Fig. 4D and Fig. S11). IL-1β showed little depletion during the 24-h time course, and appeared to equilibrate relatively rapidly in the gel with a concentration ~80% of that in the external medium (Fig. 4D). IL-1β does not bind strongly to ECM so would be expected to permeate the gel rapidly, and the lower concentration is expected from continued cellular uptake. Across almost all proteins analyzed, we found that SrtA more robustly captures dynamic changes in protein concentrations (Figs. 4D and S11). For example, the concentration of MCP-1, a chemotactic ligand for some immune cells, increases rapidly in the gel from undetectable levels at baseline to a concentration of 2000 pg/mL by 8 h after stimulation, a time point where it is undetectable in the culture supernate. Although MCP-1 appears in the culture supernate 24 h after IL-1β stimulation, its concentration was significantly lower than the parallel concentration within the gel (Fig. 4D); similar dramatic differences were seen for G-CSF, IL-2, IL-8 and others (Fig. S11). The dynamic response of MIP-1β, another well-known immune cell chemokine, illustrates the ability of SrtA-mediated dissolution to capture complex time-dependent behaviors. The local in-gel MIP-1β concentration shows a rapid increase after 8 h of stimulation, then decreases significantly by 24 h (Fig. 4D). This pattern is consistent with several possible behaviors: a burst release that saturates the system and is then rapidly consumed, induction of receptors and consequent binding and receptor-mediated degradation in response to detection of MIP-1β; or several other potential mechanisms that could be revealed in subsequent studies by analysis of the protein expression of individual cells recovered from the gel. Notably, the concentrations of MIP-1β measured in the culture supernate fail to capture this dynamic behavior – the concentration appears to increase above basal after 8 h and then continue to increase modestly up to 24 h (Fig. 4D). Other chemokines, such as IL-6 and RANTES, show a more linear lag between the in-gel and the culture supernate concentrations. Notably, basal levels for RANTES are near-zero in the culture supernate, while they are significant (200 pg/mL) in the gel (Fig. 4D). Some proteins, such as FGF, show little change upon stimulation, but are at dramatically higher concentrations in the gel than in the medium (Fig. S11).

2.6. Systems analysis of local, but not external, cytokine concentrations identifies exogenous IL-1β as central node for inflammatory cytokine response

An overarching goal of measuring local, dynamic cell-cell communication networks in 3D epithelial-stromal culture models is to build computational network models to discern disease mechanisms and potential therapeutic targets that are non-intuitive based on simple single-pathway analysis. While the experimental system described here is relatively simple in terms of cellular components (i.e., containing only stromal fibroblasts and epithelial cells and lacking the complement of immune cells present in stroma), it nevertheless provides useful data to illustrate the conceptual process of creating computational network models from dynamic profiles of paracrine signaling proteins, and the relative physiological insights that can be discerned from using data taken from the supernate measurement or the gel measurements.

We analyzed the temporal protein concentrations obtained for 27 cytokines and growth factors measured at 0, 8, and 24 h post- IL-1β stimulation by constructing separate dynamic correlation networks (DCNs) for each of the two data sets, i.e., those representing the external measurements (culture supernates) and those representing the local measurements (within gels, by gel dissolution). Dynamic correlation networks are typically used to infer transcriptional regulatory networks from longitudinal microarray data. The method computes partial correlations using shrinkage estimation, and is therefore well suited for small sample high-dimensional data. Furthermore, by computing partial correlations and correcting for multiple hypothesis testing, DCNs limit the number of indirect dependencies that appear in the network and avoid the formation of “hairball” networks. Here, we use DCNs to identify dependencies among cytokines that may indicate either functional relationships or co-regulation. Since IL-1β is known to trigger a number of chemokines and other pro-inflammatory cytokines, which can further elicit signaling cascades (e.g. IL-6, TNFα, MIPs and VEGF [60,61]), we anticipated acute stimulation by exogenous IL-1β to correlate positively with (i.e., induce upregulation of) many of the measured cytokines while suppressing others. In the DCN approach, relationships between cytokines ‘nodes’ are elucidated by calculating correlation coefficients for each pair of cytokines/nodes across the three time-points (see Methods), and then pruned to partial correlation relationship by removing indirect contributions among all potentially neighboring nodes. This DCN algorithm approach is especially useful for obtaining reliable first-order approximations of the causal structure of high-dimensionality data sets comprising small samples and sparse networks [62].

Fig. 5 shows the statistically significant dynamic correlations, both positive and negative, comparing those found for local in-gel measurements versus those found for measurements in the medium. From the local measurements, partial correlation analysis discerns a highly interconnected cluster with two large branches stemming from IL-1β – one via MIP1β and another via IL-2. In contrast, the same analysis using the measurements from the external medium does not connect these branches directly to IL-1β but instead confines its effect to a smaller set of associations, all of which are contained within the gel network. Along with other differences that can be perceived by inspection of Fig. 5, this more complete network demonstrates that the local measurements more fully capture the biological response expected from exposure to a potent inflammatory stimulus (IL-1β) compared to measurements from the culture medium. Therefore, the local in-gel measurements may be a more accurate method to reveal unknown interactions in complex 3D systems. These proof-of-principle studies with cell lines demonstrate the potential for this approach for detailed hypothesis-driven mechanistic studies with primary cells, which produce cytokines and growth factors more abundantly than cell lines [35].

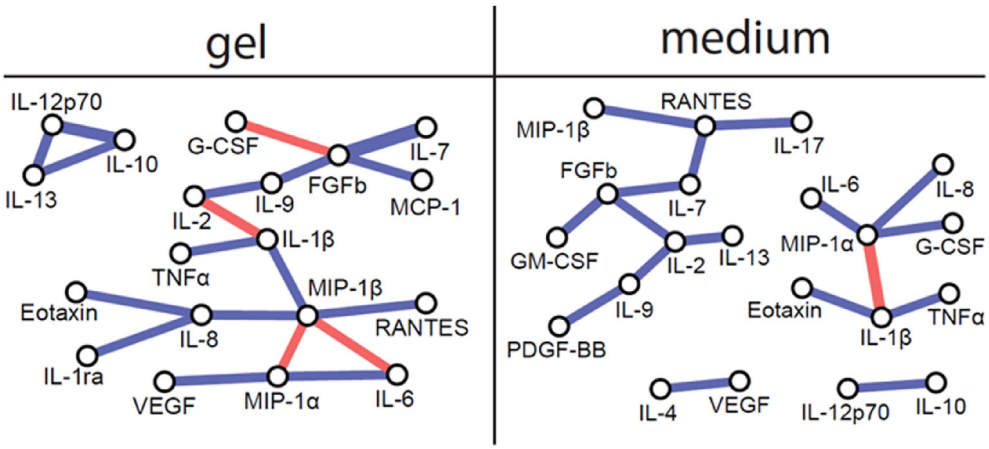

Fig. 5. Dynamic correlation networks generated from the local in-gel cytokine measurements show more extensive network compared to those generated from external medium measurements. Dynamic cytokine correlation networks constructed using either the protein measurements from the dissolved gel (left) or those made from the culture medium supernate (right) after 0, 8 and 24 h of stimulation by IL-1β. Blue edges (lines) indicate positive correlations and red edges indicate negative correlations. The edge thickness is proportional to the strength of the correlation coefficient.

3. Discussion

A barrier to productive use of 3D *in vitro* models to parse epithelial-stromal communication is access to the local cell-cell communication networks, as standard proteolytic digestion methods also degrade many target proteins (Table 1), and methods to deconstruct synthetic ECMs have limitations [14–23,63]. Here, we used the example of stromal-epithelial communication in the human endometrium to illustrate the design and implementation of a MSD- ECM that is made from readily-available or easily-synthesized reagents, can be tuned to support differentiated function in stromal-epithelial cultures, and can be dissolved rapidly on demand to release cells and proteins largely intact, before or after fixation or lysis, for further analysis by multiplex methods to yield insights into local cell-cell communication networks. We showed that an engineered version of the bacterial transpeptidase SrtA, which has been widely adapted for protein ligation reactions and can crosslink PEG macromers to encapsulate cells (Fig. S5), can be used to rapidly dissolve MSD-ECM in a cell-friendly manner (Figs. 2–3). We used a common multi-arm PEG precursor modified with a specialized adhesion motif mimicking the FN 9th-10th Type III repeats, and crosslinked gels using a peptide that can be both remodeled by cell-produced MMPs and acted on by exogenously-added SrtA, allowing both cell-mediated remodeling and on-demand dissolution.

SrtA is an attractive enzyme for dissolving gels as it is relatively small (~20 kDa), easy to produce recombinantly, and has been engineered to achieve a range of catalytic rate constants for both native and orthogonal substrates [24,27]. Importantly, the *LPXTG* motif recognized by SrtA in the first step of the transpeptidase reaction has very few known mammalian substrates [24,27,30,64] and thus can dissolve gels with minimal destruction of extracellular proteins, enabling subsequent analysis. We found that only 1 of 31 cytokines, growth factors, and MMPs was affected by SrtA dissolution (Table 1). At the time of submission, a protein BLAST search for non-redundant proteins containing the LPXTG sequence reveals that only 0.45% contain the motif, excluding hypothetical/predicted proteins in the NIH NCBI database.

The combination of gel properties, including the extent of crosslinking and the nature of the adhesion motif, fostered physiologically appropriate behavior of both epithelial and stromal cells in co-culture. Importantly, the modular synthetic ECM supported the physiological response of endometrial cells to decidualization cues (Fig. 1, Fig. S5) and was more conducive to supporting both epithelial (proper apical-basal polarization in acini) and stromal (elongation and migration) phenotypes simultaneously than the benchmark, Matrigel. These findings add to the growing literature of applications where synthetic ECMs —designed to support either stromal or epithelial cultures via modular manipulation of adhesive, mechanical, permeability, and degradation properties — are emerging to address the shortcomings of natural ECMs [1,28,31,65–69]. We also found that primary hepatocytes, which tend to lose differentiated function rapidly in culture [70], recovered from the isolation process to a highly differentiated state, as assessed by the increase in albumin production from day 1 to day 7 (Fig. S7); this analysis also demonstrated the propensity of proteins to accumulate in the gel at higher concentrations than seen in the supernate culture media outside the gel (Fig. 4). The gentle nature of the dissolution process, compared to standard proteolytic degradation processes used for deconstructing tissues containing stromal elements, where dispase is relative ineffective, enables epithelial cell-cell adhesions to stay intact and preserves cell viability after passaging (Fig. 3B–C, S6-7).

Our findings that SrtA treatment did not appear to impair cell viability and function is consistent with several other published reports using comparable concentrations and timing of SrtA exposures to effect cell surface modifications. The Liu lab, which developed the mutant sortases, demonstrated cell surface labeling of live HeLa cells engineered to express CD154 with an *LPETG* motif at the (extracellular) C-terminus using 100 μM SrtA (WT and mutant) with a 5–10 min incubation and 1 mM *GGG* substrate, with no apparent cytotoxicity [24]. Similarly, no cytotoxicity was observed when 150 μM SrtA and 5 mM *GGG* substrate was used with incubation times up to 30 min to label the surfaces of live HEK293 cells engineered to express proteins bearing an *LPETG* tag [30]. In a more sensitive test, the Ploegh lab demonstrated that incubating live mouse splenocytes for an hour with 20–40 μM WT SrtA and 0.4 mM biotinylated *LPETG* motif resulted in labeling of endogenous cell surface proteins containing N-terminal *GGG* motifs, and that when this approach was used to modify activated mouse T cells with *LPETG*-tagged single-chain antibodies, the labeled cells were viable and carried out their immune functions in

apparently normal or even enhanced fashion [64]. These published data, in aggregate with the results we report here, suggest that 20–150 μM SrtA is not only non-toxic, but appears to exert minimal influence on complex cell phenotypes.

The MSD-ECM gel dissolution process did not exhibit a strong dependence on the crosslink percentage or the sequences flanking the *LPXTG* motif (Fig. S2). Gel dissolution could also be readily accomplished following *in situ* lysis of cells or fixation of the gels, so that the cell morphologies and local cell-produced ECM were retained (Fig. 3).

Stromal-epithelial crosstalk involves a dense network of interconnected pathways, which, when perturbed, evolves rapidly by multiple mechanisms, including increased shedding of cell-surface growth factors and receptors [8,14]. Thus, while transcriptomic analysis of isolated cell populations provides some insights, discordance between mRNA levels and protein expression and protein states [71–73] – especially on the time scale of hours during shifts in state – motivate a focus on multiplex measurements of extracellular cytokines, growth factors, and other effector proteins that integrate myriad transcriptomic-level changes into concerted action. Analysis of networks of proteins and/or protein states can provide insights into complex mechanisms of therapeutic efficacy or resistance [74,75].

To illustrate how the parsing of epithelial-stromal communication networks might be improved using local in-gel measurements compared to those in the supernate outside the gel, we analyzed the response of encapsulated co-cultures of human endometrial stromal and epithelial cells to a known inflammatory cue, IL-1β, using multiplex immunobead assays to measure concentrations of 27 cytokines and growth factors and 4 MMPs following stimulation. As expected, almost all of them showed significantly higher concentrations in the local cellular environment than in the medium (Fig. 4). As the objective of making multiplex measurements is to ascertain networks of communication, we compared how the measurements from the two different compartments revealed dynamic network structure using a DCN approach (Fig. 5). This analysis revealed a complex, highly-interconnected network centered on the stimulant IL-1β when measurements of local, in-gel proteins were used for analysis, but only several sparse unconnected networks when measurements of proteins in the supernate culture medium were used. While the outcome of this analysis is circumscribed to epithelial-fibroblast interactions and does not represent the full scope of endometrial responses to inflammation involving immune cells, the results dramatically illustrate the power of local measurements to reveal physiological network behavior and motivate further work with more complex cell compositions. Furthermore, the approach described here enables cell recovery to gain multiple levels of information by complementary cell assays, such as flow cytometry studies of surface receptors and targeted intracellular proteomics and transcriptomics.

Currently, the major reason new drugs fail in the clinic is due to lack of efficacy [76], particularly in cancer and inflammatory diseases where the underlying biological mechanisms are complex and may involve re-wiring of intracellular and extracellular communication networks, or subtle differences in network operation between different patient groups [74]. Often, drugs target a single pathway, which can have unintended consequences when other pathways in the network compensate or overcompensate [14,74,77], underscoring the need for new approaches to unravel network behavior in response to perturbations. The powerful tools developed here have the potential to enable studies of such re-wiring events to better understand complex networks and pathologies, and to better inform the drug development process.

4. Conclusion

The MSD-ECM approaches described herein should have broad applicability to examination of communication networks in cancer, chronic inflammation, and other complex diseases where local communication is multifaceted and dynamic. Although we used a standard multiplex immunobead assay for discerning a modest number of components as an illustration, this approach could productively be combined with a recently-described cell-specific proteomics [8] to gain extraordinary insight into the details of dynamic network operation. Further, the observation that fixed gels can release cells with the local cell morphology and pericellular environment intact suggests that some degree of insight into spatial enrichment of particular molecules can be discerned, via standard immunostaining or by combining immunostaining with high-resolution single cell analysis [78]; such analysis could yield interesting insights into combinations of receptor-ligand pairings. Although we employed a PEG-based synthetic ECM gel for the MSD-ECM formulation used in this work, we expect that any hydrogel crosslinked with peptides that incorporate the *LPXTG* motif could be dissolved by this approach.

In summary, we have described a new approach to creating and probing complex, 3D human heterotypic cell cultures, with reagents that are highly accessible, reproducible, and amenable to modular tuning for specific culture compositions.

5. Materials and methods

5.1. Peptides and functionalized polymers

8-arm PEG vinyl sulfone MW 40,000 Da (PEG-VS) and 8-arm PEG norbornene MW 20,000 Da (PEG-NB) were purchased from JenKem Technology (Beijing). The following peptides were custom-synthesized by Boston Open Labs (Cambridge, MA): the cross-linking peptides GCRD-LPRTG-GPQGIWGQ-DRCG (LW-XL) and GCRD-LPRTG-GPQGIAGQ-DRCG (LA-XL), the adhesive peptides PHSRNGGGK-GGGERCG-GGRGDSPY (*PHSRN-K-RGD*) and PHSRNGGGK-(fluorescein)GGGERCG-GGRGDSPY (*F-PHSRN-K-RGD*). All amine terminals were acetylated and all carboxyl terminals were amidated.

5.2. Sortase expression

Sortase A pentamutant (P94R/D160N/D165A/K190E/K196T) (plasmids were gift from Dr. David Liu) was expressed and purified as previously reported [24,79]. Briefly, BL21 *E. coli* glycerol stocks transformed with pET29 sortase expression plasmids were cultured at 37 °C in 5 mL LB media supplemented with 30 μg/mL kanamycin overnight. The tubes were then each transferred to 1 L of LB and 30 μg/mL kanamycin and grown for 3–4 h until OD was 0.4–0.6. 1 mM IPTG was added to induce protein expression overnight at room temperature. Cells were harvested by centrifugation and washed with lysis buffer (50 mM Tris-HCl, 150 mM NaCl, 10% (vol/vol) glycerol, 10 mM imidazole, 1 mg/mL lysozyme, 0.25% β-mercaptoethanol, EDTA-free protease inhibitor cocktail set III (Calbiochem)). Cells were lysed by sonication, centrifuged, and the resulting clarified supernatant was purified with Ni-NTA agarose columns. Elution fractions were checked for purity using SDS-PAGE. Clean elution fractions were consolidated, dialyzed against 50 mM Tris-HCl and 150 mM NaCl (pH 7.5), then concentrated with Ultra-15 Centrifugal Filter Units (Amicon). Aliquots were sterile filtered using a 0.1 μm filter and flash frozen for long-term storage at −80 °C. Final enzyme concentration was calculated by measuring A_{280} and using the extinction coefficient of 17420$M^{-1}cm^{-1}$ [80].

5.3. Cell culture of endometrial cells

Ishikawa human endometrial adenocarcinoma cells (Sigma-Aldrich) and hTERT-immortalized human endometrial stromal cells (tHESCs) (ATCC) were routinely cultured in a humidified atmosphere at 37 °C and 5% CO_2 in phenol red free DMEM/F12 mixture of Dulbecco's Modified Eagle's Medium and Ham's F-12 (Gibco) media supplemented with 1% penicillin/streptomycin (Gibco) and 10% *v*/*v* dextran/charcoal treated fetal bovine serum (Atlanta Biologicals) (DMEM/F12/FBS). Epithelial cells were split 1:4 and stromal cells were split 1:2 once they reached 70–80% confluency, and medium was replaced every 2–3 days. Following reports of possible contamination of endometrial cell lines by HeLa or other lines [81], STR profiling analysis (Genetic Resources Core Facility, Johns Hopkins School of Medicine, Institute of Genetic Medicine) was used to confirm the fidelity of the tHESCs and Ishikawa cell lines against known cell databanks. Cell lines were routinely used prior to passage 10. Primary stromal cells used in decidualization experiments were acquired as described in Ref. [13]. Participants were recruited through Newton-Wellesley Hospital and provided informed consent in accordance with an IRB protocol approved by the Partners Human Research Committee, and samples were analyzed at MIT in accordance with a protocol approved by the Massachusetts Institute of Technology Committee on the Use of Humans as Experimental Subjects.

5.4. PEG norbornene (PEG-NB) hydrogel synthesis for dissolution rate quantification

Hydrogels of 18 μL were fabricated in a one-pot synthesis using norbornene/thiol-ene click chemistry inside a 1 mL syringe from which the tip was cut off at the 0.1 mL mark. 4 wt% PEG-NB was crosslinked with the dithiol peptide LW-XL at a stoichiometric ratio (r) of 0.55 thiols per norbornene unless otherwise indicated. The adhesive peptide (*PHSRN-K-RGD*) was incorporated at 500 μM nominal concentration. For quantification of macromer release during gel dissolution characterization experiments, 14% of *PHSRN-K-RGD* was fluorescein-labeled (*F-PHSRN-K-RGD*). IRGACURE 2959 (Ciba, Prod. No. 0298913AB) was included at 0.08 wt% and the precursor solution was UV-irradiated for 5 s at ~800 mW/cm^2. The hydrogels were placed in a 24-well plate with 600 μL DMEM/F12/FBS per well and allowed to swell overnight in a humidified atmosphere at 37 °C and 5% CO_2 to emulate culture conditions.

5.5. 3D stromal and epithelial (cell lines) co-culture cell encapsulation in PEG-VS hydrogels for (Luminex) signaling studies

Hydrogels of 25 μL were fabricated using Michael-type reaction chemistry inside a 1 mL from which the tip was cut off at the 0.1 mL mark. Briefly, peptide-functionalized macromers were prepared by reacting PEG-VS (7.2 mM) with free thiols (−SH) on adhesion peptides in 1x PBS with 1 M HEPES (pH 7.8) for 30 min. Immediately after the functionalization reaction, the peptide-functionalized PEG-VS (fPEG-VS) macromer (average 6.4 free −VS groups per macromer) solution was mixed with a cell suspension of 1:1 stromal and epithelial cells (13.49×10^6 cells/mL in PBS). Peptide-functionalized 8-arm PEG-VS macromers were then reacted with the cysteine thiol (−SH) groups on the bifunctional sortase and MMP sensitive peptide crosslinker LA-XL in volumetric ratios of 4.9:8.6:1 fPEG-VS:cells:LW-XL to yield a final crosslinking solution comprising 8×10^6 cell/mL (200,000 cells in 25 μL), 2 mM total adhesion peptide, 1.2 mM total PEG macromers (5 wt%), and 2.5 mM crosslinking peptide in PBS, 1 M HEPES buffer (pH 7.8). Nominal adhesive peptide concentrations in the final gel was 2 mM *PHSRN-K-RGD*. After pipetting the mixture up and down for 2 min, 25 μL was pipetted onto each syringe. The solutions were allowed to gel (~6 additional minutes) and were incubated at RT for 15 min to allow crosslinking to proceed to completion. After gelation was complete, the gels were moved to 24 well plates and 400 μL of DMEM/F12/FBS was added to each gel. Cultures were maintained in a humidified incubator at 37 °C, 95% air, 5% CO_2.

5.6. Hydrogel dissolution quantification

18 μL PEG-NB or PEG-VS hydrogels were synthesized as described above and allowed to swell in a humidified atmosphere at 37 °C and 5% CO_2 for 24 h in DMEM/F12/FBS. Swollen gels (~25 μL swollen volume) were removed from the media using a spatula and transferred into a 1.6 mL Eppendorf tube. A 60 μL solution of sortase A penta-mutant P94R/D160N/D165A/K190E/K196T (SrtA), expressed and purified as previously reported [24,28,29], and Gly-Gly-Gly (*GGG*) (Sigma-Aldrich) in DMEM/F12/FBS was added to the hydrogel in the Eppendorf tube at 50 μM and 18 mM respectively unless otherwise specified. Where indicated, SrtA was added for 10 min or 30 min and incubated at 37 °C prior to adding GGG. Upon addition of both SrtA and GGG, the tubes were placed on a thermal shaker and mixed at 300 RPM during gel dissolution. At each of the time points indicated in the plots, 2 μL were removed from the gel-containing tubes and added to 38 μL of 50 μM HEPES buffer in a 384-well plate. Fluorescence ($\lambda_{ex} = 485$ nm, $\lambda_{em} = 525$ nm) of each time point sample was measured using a microplate reader (SpectraMax M2^e, Molecular Devices). Each time point was normalized to their respective hydrogel dissolved solution that had been dissolved for at least 2 h. A fluorescein linear standard curve containing 0, 20, 50, 100, or 250 μM was established to ensure the fluorescence measurements for each time point were in a linear range.

5.7. Determination of soluble cytokine depletion by SrtA, trypsin, and Liberase™ through Luminex

A solution of 27 cytokine recombinant standards of known concentrations (67 μL) from a Bio-Plex Pro human cytokine 27-plex assay (Bio-Rad, #M500KCAF0Y) were incubated with 14 μL of SrtA (10, 30, or 50 μM final), GGG (9 or18 mM final), SrtA + GGG (50 μM + 18 mM, or 30 μM + 9 mM final, respectively), trypsin (1X = 0.25% final) (Gibco, Ref 15,090-046), Liberase™ (10 μg/mL final) (Roche, Ref. 05401119001), or a buffer control (50 mM HEPES, 150 mM NaCl, 10 mM CaCl2, pH 7.9). After a 45 min incubation, 8.1 μL of protease inhibitor cocktail (Roche, Prod. No. 05892953001) were added to all conditions for a final concentration of 5 mg/mL, as recommended by the vendor. The cytokine concentrations after treatment were measured by Luminex assay as described below. Data reported as percent decrease compared to the buffer control.

5.8. IL-1β stimulation of endometrial epithelial/stromal co-cultures

Endometrial co-cultures were encapsulated as described above (t = −24 h) and allowed to equilibrate in DMEM/F12/FBS 24 h. At t = 0 h, 10 ng/mL of IL-1β was added to some conditions. Gels with and without IL-1β stimulation were sacrificially dissolved to assess the concentration of a number of cytokines inside and outside the gel (see below) 8 h and 24 h after IL-1β stimulation.

5.9. Multiplex measurement of protein concentrations inside hydrogel and in culture media of 3D epithelial/stromal co-culture

Epithelial and stromal cell co-cultures were encapsulated in PEG-VS as described above in 25 μL hydrogels cultured in 400 μL of DMEM/F12/FBS. Blank PEG-VS gels (hydrogels of the same exact

composition but with no cells) were fabricated at the same time and submerged in 400 μL of 50 mM HEPES, 150 mM NaCl, 10 mM CaCl2, pH 7.9. At the time points indicated, the co-culture and blank gels were removed from the culture media, transferred into Eppendorf tubes, and their weight was recorded to estimate their volume for future dilution correction of cytokine concentrations (swollen gels were ~60 μL). Co-culture gels were dissolved in 90 μL of SrtA and GGG at 50 μM and 18 mM final concentrations (accounting for gel volume), respectively at 37 °C in 50 mM HEPES, 150 mM NaCl, 10 mM $CaCl_2$. To favor homogeneous dissolution, hydrogels were infused with 76.5 μL SrtA for 10 min at 37 °C prior to adding GGG (13.5 μL). Simultaneously, 60 μL of culture media from each co-culture gel were added to blank gels, and then 30 μL of SrtA and GGG at 50 μM and 18 mM final concentrations (accounting for gel volume) respectively were added at 37 °C in 50 mM HEPES, 150 mM NaCl, 10 mM $CaCl_2$. Co-culture gels and their respective media were diluted equivalently in the dissolution process. Dissolution was allowed to take place on a thermal shaker with gentle mixing at 300 RPM. Upon gel dissolution (8–10 min), the dissolved-gel solutions/cell suspensions were spun down for 3.5 min at 350 RCFs and the supernate for each sample was transferred into a new tube to remove the cells prior to soluble cytokine measurements. 10 μL of protease inhibitor cocktail (Roche, Prod. No. 05892953001) was added to all conditions for a final concentration of 5 mg/mL, as recommended by the vendor prior to Luminex assay cytokine quantification.

5.10. Statistical analysis

Means for in gel vs medium protein concentrations (Fig. 4) were compared at each time point independently using Holm-Sidak method for multiple comparisons using GraphPad Prism with $\alpha = 5.00\%$.

5.11. Dynamic correlation networks (DCNs)

DCNs for cell-cell communication in the co-cultures based on either local (in-gel) or external (culture medium) for the co-culture gels and co-culture gel media with dissolved blank gels were constructed using cytokine concentrations at 0, 8, and 24 h post IL-1β stimulation. From the cytokine time-course measurements (three biological replicates and three technical replicates per biological replicate), dynamic partial correlation coefficients, ρ_{ij}, were calculated using the procedure described in Ref. [62] and implemented in the GeneNet package (version 1.2.13) in R (version 3.2.3) here: https://CRAN.R-project.org/package=GeneNet. Briefly, two cytokines have a positive dynamic correlation if both time-courses tend to be on the same side of their time-average (the average value at a given time-point), or a negative dynamic correlation if they tend to be on opposite sides of their time average. An adjacency matrix defining the connections between cytokines was then constructed using partial correlation coefficients with an absolute value greater than 0.2 as follows:

$$A_{ij} = \rho_{ij}^{\alpha}$$

with $\alpha = 6$.

Conflict of interest

The authors confirm that there are no known conflicts of interest associated with this publication and there has been no significant financial support for this work that could have influenced its outcome.

Author contributions

J.V., C.C., C.C.A., A.W., A.B., D.R., E.G., D.L., B.I., F.W., and L.G., designed research; J.V., C.C., A.W., A.B., L.S., and D.R. performed research; J.V., A.W. and K.R. contributed new reagents; J.V., A.W. and M.K. analyzed data; and J.V., C.C., M.K. and L.G wrote the paper.

Acknowledgements

We gratefully acknowledge Prof. David Liu (Harvard University) for sortase mutant plasmids. The authors would like to acknowledge the study and surgical staff and patients that agreed to participate through Newton-Wellesley Hospital, including Drs. Keith Isaacson and Stephanie Morris, and for clinical and experimental technical support from Julia Papps at MIT. We also acknowledge Prof. Barbara Imperiali (MIT) for many helpful conversations about sortase and other facets of chemistry used herein. This work was supported by NIH R01EB010246, NIH UH2TR000496, the Institute for Collaborative Biotechnologies (W911NF-09-0001), NIH T32GM008334, the DARPA Microphysiological Systems Program (W911NF-12-2-0039), the John and Karine Begg Fund to the Center for Gynepathology Research, the Begg New Horizon Fund for Undergraduate Research at MIT, the Biophysical Instrumentation Facility, The Manton Foundation, the Ludwig Postdoctoral Fellowship for Cancer Research for E.G. and a Swiss National Science Foundation Postdoctoral Fellowship for K.R. We thank the Koch Institute Swanson Biotechnology Center for microscopy core facilities.

Appendix A. Supplementary data

Supplementary data related to this article can be found at http://dx.doi.org/10.1016/j.biomaterials.2017.03.030.

References

[1] M.P. Lutolf, J.A. Hubbell, Synthetic biomaterials as instructive extracellular microenvironments for morphogenesis in tissue engineering, Nat. Biotechnol. 23 (1) (2005) 47–55.
[2] J.A. Burdick, W.L. Murphy, Moving from static to dynamic complexity in hydrogel design, Nat. Commun. 3 (2012) 1269.
[3] L.G. Griffith, M.A. Swartz, Capturing complex 3D tissue physiology in vitro, Nat. Rev. Mol. Cell Biol. 7 (3) (2006) 211–224.
[4] B. Trappmann, et al., Extracellular-matrix tethering regulates stem-cell fate, Nat. Mater 11 (7) (2012) 642–649.
[5] A.J. Engler, S. Sen, H.L. Sweeney, D.E. Discher, Matrix elasticity directs stem cell lineage specification, Cell 126 (4) (2006) 677–689.
[6] T.L. Anderson, F. Gorstein, K.G. Osteen, Stromal-epithelial cell communication, growth factors, and tissue regulation, Lab. Invest. 62 (5) (1990) 519–521.
[7] J.M. Rothberg, M. Sameni, K. Moin, B.F. Sloane, Live-cell imaging of tumor proteolysis: impact of cellular and non-cellular microenvironment, Biochim. Biophys. Acta 1824 (1) (2012) 123–132.
[8] C.J. Tape, et al., Oncogenic KRAS regulates tumor cell signaling via stromal reciprocation, Cell 165 (7) (2016) 1818.
[9] H. Choi, et al., Transcriptome analysis of individual stromal cell populations identifies stroma-tumor crosstalk in mouse lung cancer model, Cell Rep. 10 (7) (2015) 1187–1201.
[10] K.O. Osuala, et al., Il-6 signaling between ductal carcinoma in situ cells and carcinoma-associated fibroblasts mediates tumor cell growth and migration, BMC Cancer 15 (2015) 584.
[11] T. Kurita, et al., The activation function-1 domain of estrogen receptor alpha in uterine stromal cells is required for mouse but not human uterine epithelial response to estrogen, Differentiation 73 (6) (2005) 313–322.
[12] K.G. Osteen, et al., Stromal-epithelial interaction mediates steroidal regulation of metalloproteinase expression in human endometrium, Proc. Natl. Acad. Sci. U. S. A. 91 (21) (1994) 10129–10133.
[13] K.G. Osteen, G.A. Hill, J.T. Hargrove, F. Gorstein, Development of a method to isolate and culture highly purified populations of stromal and epithelial cells from human endometrial biopsy specimens, Fertil. Steril. 52 (6) (1989) 965–972.
[14] M.A. Miller, et al., ADAM-10 and -17 regulate endometriotic cell migration via concerted ligand and receptor shedding feedback on kinase signaling, Proc. Natl. Acad. Sci. U. S. A. 110 (22) (2013) E2074–E2083.
[15] L.J. McCawley, P. O'Brien, L.G. Hudson, Epidermal growth factor (EGF)- and

scatter factor/hepatocyte growth factor (SF/HGF)- mediated keratinocyte migration is coincident with induction of matrix metalloproteinase (MMP)-9, J. Cell Physiol. 176 (2) (1998) 255–265.
[16] A. Petrelli, et al., Ab-induced ectodomain shedding mediates hepatocyte growth factor receptor down-regulation and hampers biological activity, Proc. Natl. Acad. Sci. U. S. A. 103 (13) (2006) 5090–5095.
[17] M.A. Brown, et al., The use of mild trypsinization conditions in the detachment of endothelial cells to promote subsequent endothelialization on synthetic surfaces, Biomaterials 28 (27) (2007) 3928–3935.
[18] Y. Lei, D.V. Schaffer, A fully defined and scalable 3D culture system for human pluripotent stem cell expansion and differentiation, Proc. Natl. Acad. Sci. U. S. A. 110 (52) (2013) E5039–E5048.
[19] J. Zhang, A. Skardal, G.D. Prestwich, Engineered extracellular matrices with cleavable crosslinkers for cell expansion and easy cell recovery, Biomaterials 29 (34) (2008) 4521–4531.
[20] T. Billiet, M. Vandenhaute, J. Schelfhout, S. Van Vlierberghe, P. Dubruel, A review of trends and limitations in hydrogel-rapid prototyping for tissue engineering, Biomaterials 33 (26) (2012) 6020–6041.
[21] C.A. DeForest, K.S. Anseth, Photoreversible patterning of biomolecules within click-based hydrogels, Angew. Chem. Int. Ed. Engl. 51 (8) (2012) 1816–1819.
[22] M.W. Tibbitt, A.M. Kloxin, K.S. Anseth, Modeling controlled photodegradation in optically thick hydrogels, J. Polym. Sci. A Polym. Chem. 51 (9) (2013) 1899–1911.
[23] L.D. Amer, A. Holtzinger, G. Keller, M.J. Mahoney, S.J. Bryant, Enzymatically degradable poly(ethylene glycol) hydrogels for the 3D culture and release of human embryonic stem cell derived pancreatic precursor cell aggregates, Acta Biomater. 22 (2015) 103–110.
[24] I. Chen, B.M. Dorr, D.R. Liu, A general strategy for the evolution of bond-forming enzymes using yeast display, Proc. Natl. Acad. Sci. U. S. A. 108 (28) (2011) 11399–11404.
[25] J.M. Antos, et al., Site-specific N- and C-Terminal labeling of a single polypeptide using sortases of different specificity, J. Am. Chem. Soc. (2009) 10800–10801.
[26] M.W. Popp, H.L. Ploegh, Making and breaking peptide bonds: protein engineering using sortase, Angew. Chem. Int. Ed. Engl. 50 (22) (2011) 5024–5032.
[27] B.M. Dorr, H.O. Ham, C. An, E.L. Chaikof, D.R. Liu, Reprogramming the specificity of sortase enzymes, Proc. Natl. Acad. Sci. U. S. A. 111 (37) (2014) 13343–13348.
[28] E. Cambria, et al., Covalent modification of synthetic hydrogels with bioactive proteins via sortase-mediated ligation, Biomacromolecules 16 (8) (2015) 2316–2326.
[29] A.T. Krueger, C. Kroll, E. Sanchez, L.G. Griffith, B. Imperiali, Tailoring chimeric ligands for studying and biasing ErbB receptor family interactions, Angewandte Chemie Int. Ed. Engl. 53 (10) (2014) 2662–2666.
[30] M.W. Popp, J.M. Antos, G.M. Grotenbreg, E. Spooner, H.L. Ploegh, Sortagging: a versatile method for protein labeling, Nat. Chem. Biol. 3 (11) (2007) 707–708.
[31] N.O. Enemchukwu, et al., Synthetic matrices reveal contributions of ECM biophysical and biochemical properties to epithelial morphogenesis, J. Cell Biol. 212 (1) (2016) 113–124.
[32] E.B. Peters, N. Christoforou, K.W. Leong, G.A. Truskey, J.L. West, Poly(ethylene glycol) hydrogel scaffolds containing cell-adhesive and protease-sensitive peptides support microvessel formation by endothelial progenitor cells, Cell Mol. Bioeng. 9 (1) (2016) 38–54.
[33] B.V. Sridhar, et al., Development of a cellularly degradable PEG hydrogel to promote articular cartilage extracellular matrix deposition, Adv. Healthc. Mater 4 (5) (2015) 702–713.
[34] K. Bott, et al., The effect of matrix characteristics on fibroblast proliferation in 3D gels, Biomaterials 31 (32) (2010) 8454–8464.
[35] C. Cook, et al., Local remodeling of synthetic extracellular matrix microenvironments by Co-cultured endometrial epithelial and stromal cells enables long-term dynamic physiological function, Integr. Biol. (2017), http://dx.doi.org/10.1039/c6ib00245e.
[36] W. Kuhlman, I. Taniguchi, L.G. Griffith, A.M. Mayes, Interplay between PEO tether length and ligand spacing governs cell spreading on RGD-modified PMMA-g-PEO comb copolymers, Biomacromolecules 8 (10) (2007) 3206–3213.
[37] D.J. Irvine, K.A. Hue, A.M. Mayes, L.G. Griffith, Simulations of cell-surface integrin binding to nanoscale-clustered adhesion ligands, Biophys. J. 82 (1 Pt 1) (2002) 120–132.
[38] M. Kreiner, et al., Self-assembling multimeric integrin alpha5beta1 ligands for cell attachment and spreading, Protein Eng. Des. Sel. 21 (9) (2008) 553–560.
[39] J.L. Sechler, S.A. Corbett, J.E. Schwarzbauer, Modulatory roles for integrin activation and the synergy site of fibronectin during matrix assembly, Mol. Biol. Cell 8 (12) (1997) 2563–2573.
[40] A.C. Brown, M.M. Dysart, K.C. Clarke, S.E. Stabenfeldt, T.H. Barker, Integrin alpha3beta1 binding to fibronectin is dependent on the ninth type III repeat, J. Biol. Chem. 290 (42) (2015) 25534–25547.
[41] J.T. Arnold, D.G. Kaufman, M. Seppala, B.A. Lessey, Endometrial stromal cells regulate epithelial cell growth in vitro: a new co-culture model, Hum. Reprod. 16 (5) (2001) 836–845.
[42] J.T. Arnold, B.A. Lessey, M. Seppala, D.G. Kaufman, Effect of normal endometrial stroma on growth and differentiation in Ishikawa endometrial adenocarcinoma cells, Cancer Res. 62 (1) (2002) 79–88.
[43] H.K. Kleinman, G.R. Martin, Matrigel: basement membrane matrix with biological activity, Semin. Cancer Biol. 15 (5) (2005) 378–386.
[44] M.P. Lutolf, J.A. Hubbell, Synthesis and physicochemical characterization of end-linked poly(ethylene glycol)-co-peptide hydrogels formed by Michael-type addition, Biomacromolecules 4 (3) (2003) 713–722.
[45] M.P. Lutolf, N. Tirelli, S. Cerritelli, L. Cavalli, J.A. Hubbell, Systematic modulation of michael-type reactivity of thiols through the use of charged amino acids, Bioconjug. Chem. (2001) 1051–1056.
[46] J.J. Brosens, N. Hayashi, J.O. White, Progesterone receptor regulates decidual prolactin expression in differentiating human endometrial stromal cells, Endocrinology 140 (10) (1999) 4809–4820.
[47] B. Gellersen, J. Brosens, Cyclic AMP and progesterone receptor cross-talk in human endometrium: a decidualizing affair, J. Endocrinol. 178 (3) (2003) 357–372.
[48] E.G. Erdos, R.A. Skidgel, Neutral endopeptidase 24.11 (enkephalinase) and related regulators of peptide hormones, FASEB J. 3 (2) (1989) 145–151.
[49] Popp MW-L, Antos JM, & Ploegh HL (2009) Site-specific protein labeling via sortase-mediated transpeptidation. Current protocols in protein science/editorial board, John E. Coligan... [et al.] Chapter 15:Unit 15.13-Unit 15.13.
[50] C.E. Gargett, K.E. Schwab, R.M. Zillwood, H.P. Nguyen, D. Wu, Isolation and culture of epithelial progenitors and mesenchymal stem cells from human endometrium, Biol. Reprod. 80 (6) (2009) 1136–1145.
[51] C.A. Gedye, et al., Cell surface profiling using high-throughput flow cytometry: a platform for biomarker discovery and analysis of cellular heterogeneity, PLoS One 9 (8) (2014) e105602.
[52] Y. Kitano, N. Okada, Separation of the epidermal sheet by dispase, Br. J. Dermatol 108 (5) (1983) 555–560.
[53] J.A. Keenan, T.T. Chen, N.L. Chadwell, D.S. Torry, M.R. Caudle, IL-1 beta, TNF-alpha, and IL-2 in peritoneal fluid and macrophage-conditioned media of women with endometriosis, Am. J. Reprod. Immunol. 34 (6) (1995) 381–385.
[54] S.D. Spandorfer, et al., Interleukin-1 levels in the supernatant of conditioned media of embryos grown in autologous endometrial coculture: correlation with outcome after in vitro fertilization, Am. J. Reprod. Immunol. 43 (1) (2000) 6–11.
[55] F. Raga, E.M. Casan, F. Bonilla-Musoles, Gonadotropin-releasing hormone (GnRH)-I regulation of interleukin (IL)-1b and IL-1 receptor antagonist expression in cultured human endometrial stromal cells, J. Obstet. Gynaecol. Res. 34 (4) (2008) 464–472.
[56] S. Guay, A. Akoum, Stable inhibition of interleukin 1 receptor type II in Ishikawa cells augments secretion of matrix metalloproteinases: possible role in endometriosis pathophysiology, Reproduction 134 (3) (2007) 525–534.
[57] D. Clarke, O. Katoh, R.V. Gibbs, S.D. Griffiths, M.Y. Gordon, Interaction of interleukin 7 (IL-7) with glycosaminoglycans and its biological relevance, Cytokine 7 (4) (1995) 325–330.
[58] L. Ramsden, C.C. Rider, Selective and differential binding of interleukin (IL)-1 alpha, IL-1 beta, IL-2 and IL-6 to glycosaminoglycans, Eur. J. Immunol. 22 (11) (1992) 3027–3031.
[59] R.S. Mummery, C.C. Rider, Characterization of the heparin-binding properties of IL-6, J. Immunol. 165 (10) (2000) 5671–5679.
[60] A. Basu, J.K. Krady, S.W. Levison, Interleukin-1: a master regulator of neuroinflammation, J. Neurosci. Res. 78 (2) (2004) 151–156.
[61] J.R. Tisoncik, et al., Into the eye of the cytokine storm, Microbiol. Mol. Biol. R. 76 (1) (2012) 16–32.
[62] R. Opgen-Rhein, Korbinian Strimmer, Inferring gene dependency networks from genomic longitudinal data: a functional data approach, RevStat 4 (1) (2006) 53–65.
[63] D. Bourboulia, W.G. Stetler-Stevenson, Matrix metalloproteinases (MMPs) and tissue inhibitors of metalloproteinases (TIMPs): positive and negative regulators in tumor cell adhesion, Semin. Cancer Biol. 20 (3) (2010) 161–168.
[64] L.K. Swee, S. Lourido, G.W. Bell, J.R. Ingram, H.L. Ploegh, One-step enzymatic modification of the cell surface redirects cellular cytotoxicity and parasite tropism, ACS Chem. Biol. 10 (2) (2015) 460–465.
[65] S.P. Singh, et al., A synthetic modular approach for modeling the role of the 3D microenvironment in tumor progression, Sci. Rep. 5 (2015) 17814.
[66] C. Yang, et al., Spatially patterned matrix elasticity directs stem cell fate, Proc. Natl. Acad. Sci. U. S. A. 113 (31) (2016) E4439–E4445.
[67] M. Guvendiren, J.A. Burdick, Engineering synthetic hydrogel microenvironments to instruct stem cells, Curr. Opin. Biotechnol. 24 (5) (2013) 841–846.
[68] P.J. Wrighton, et al., Signals from the surface modulate differentiation of human pluripotent stem cells through glycosaminoglycans and integrins, Proc. Natl. Acad. Sci. U. S. A. 111 (51) (2014) 18126–18131.
[69] E. Fong, S. Tzlil, D.A. Tirrell, Boundary crossing in epithelial wound healing, Proc. Natl. Acad. Sci. U. S. A. 107 (45) (2010) 19302–19307.
[70] M.R. Ebrahimkhani, J.A. Neiman, M.S. Raredon, D.J. Hughes, L.G. Griffith, Bioreactor technologies to support liver function in vitro, Adv. Drug Deliv. Rev. 69–70 (2014) 132–157.
[71] Y. Liu, A. Beyer, R. Aebersold, On the dependency of cellular protein levels on mRNA abundance, Cell 165 (3) (2016) 535–550.
[72] T. Shi, et al., Conservation of protein abundance patterns reveals the regulatory architecture of the EGFR-MAPK pathway, Sci. Signal 9 (436) (2016) rs6.
[73] I. Kosti, N. Jain, D. Aran, A.J. Butte, M. Sirota, Cross-tissue analysis of gene and protein expression in normal and cancer tissues, Sci. Rep. 6 (2016) 24799.
[74] M.A. Miller, et al., Reduced proteolytic shedding of receptor tyrosine kinases is a post-translational mechanism of kinase inhibitor resistance, Cancer Discov. 6 (4) (2016) 382–399.
[75] P.K. Kreeger, D.A. Lauffenburger, Cancer systems biology: a network modeling perspective, Carcinogenesis 31 (1) (2010) 2–8.

[76] J. Arrowsmith, Trial watch: phase II failures: 2008-2010, Nat. Rev. Drug Discov. 10 (5) (2011) 328–329.
[77] J.R. Pritchard, D.A. Lauffenburger, M.T. Hemann, Understanding resistance to combination chemotherapy, Drug Resist Updat 15 (5–6) (2012) 249–257.
[78] C.T. Leung, J.S. Brugge, Outgrowth of single oncogene-expressing cells from suppressive epithelial environments, Nature 482 (7385) (2012) 410–413.
[79] C.P. Guimaraes, et al., Site-specific C-terminal and internal loop labeling of proteins using sortase-mediated reactions, Nat. Protoc. 8 (9) (2013) 1787–1799.
[80] R.G. Kruger, et al., Analysis of the substrate specificity of the Staphylococcus aureus sortase transpeptidase SrtA, Biochemistry 43 (6) (2004) 1541–1551.
[81] C. Korch, et al., DNA profiling analysis of endometrial and ovarian cell lines reveals misidentification, redundancy and contamination, Gynecol. Oncol. 127 (1) (2012) 241–248.